

Title	High pressure equipments in Abu-yama seismological observatory of Kyoto University
Author(s)	Kiyama, Ryo
Citation	The Review of Physical Chemistry of Japan (1956), 26(1): 24-39
Issue Date	1956-08-30
URL	http://hdl.handle.net/2433/46737
Right	
Type	Departmental Bulletin Paper
Textversion	publisher

HIGH PRESSURE EQUIPMENTS IN ABU-YAMA SEISMOLOGICAL OBSERVATORY OF KYOTO UNIVERSITY

BY RYO KIYAMA

High pressure equipments were set in Abu-yama Seismological Observatory (Director, Prof. K. Sassa) for the main object of geophysical studies of the Institutional Research "On the flow and fracture of rocks (1955)". They were designed and constructed by the hands of the researchers in the Laboratory of Physical Chemistry of Kyoto University.

Before the test working of the equipments, the outline of the equipments and the results of experiments for demonstration is mentioned in the present paper, including the high pressure works performed in the Laboratory of Physical Chemistry from 1944 up to date.

The main object of the new equipments is the measurement of behaviors of rocks which are hydrostatically compressed to the same condition as that of earth crust at nearly 100 km under the ground. The working pressure of the equipments is $30,000 \text{ kg/cm}^2$ and the inner diameter of the largest pressure chamber is 30 mm. The ranges of pressure and temperature in measurements will be extended with the progress of the research, depending on the improvement of the design and materials of the high pressure chamber.

We completed in 1944 the design and construction of the $5,000 \text{ kg/cm}^2$ gas compressor under the support of various fields, in spite of many difficulties in the World War II where pure science was ignored. This apparatus was possessed by the Physico-Chemical Society of Japan and the construction was performed under the direction of the President of the Society, Prof. Emeritus, Dr. S. Horiba, M. J. A., who was the director of the Laboratory of Physical Chemistry at that time.

The physico-chemical problems under high pressure have been studied chiefly in the Laboratory of Physical Chemistry of Kyoto University.

The high pressure works up to $15,000 \text{ kg/cm}^2$ performed by these high pressure apparatus in the Laboratory have been reported in the Review of Physical Chemistry of Japan and the list of their contents is as follows.

Apparatus

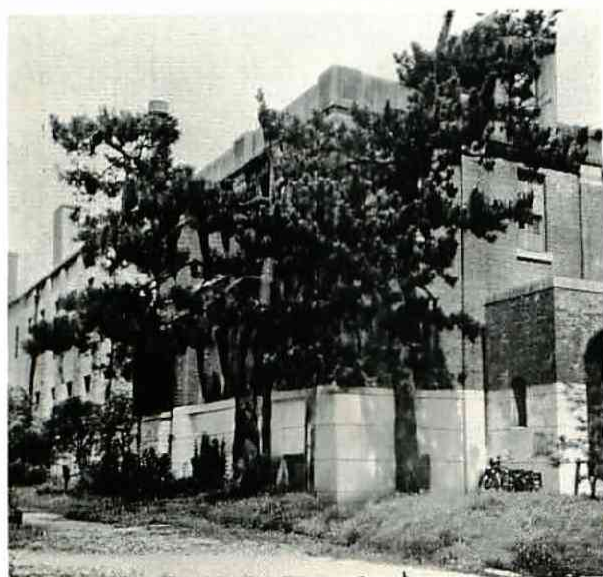
Ultra pressure, I	Making of a gas compressor and a reaction vessel for an ultra pressure	19, 1 (1945)
Ultra pressure, II	Pressure-proof electrode	19, 12 (1945)
Ultra pressure, III	Pressure-proof character of optical window	19, 17 (1945)
Ultra pressure, IV	Packing	19, 21 (1945)



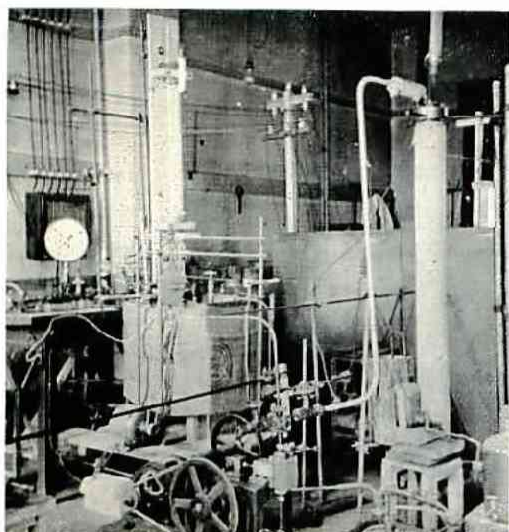
Exterior view of high
pressure laboratory of
Abu-yama Observatory



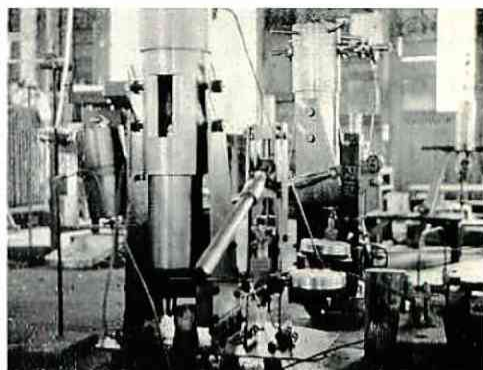
A part of high pressure
equipments of Abu-yama
Observatory



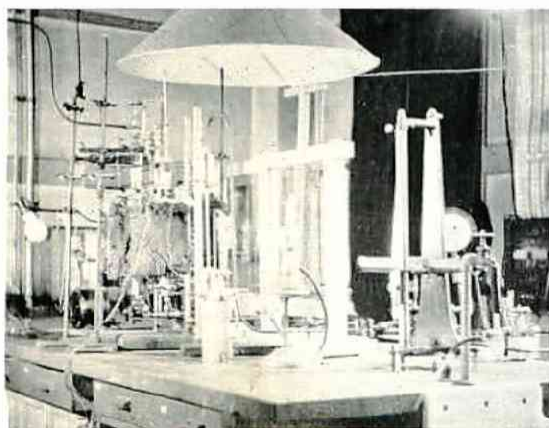
Exterior view of Laboratory
of Physical Chemistry for
high pressure research



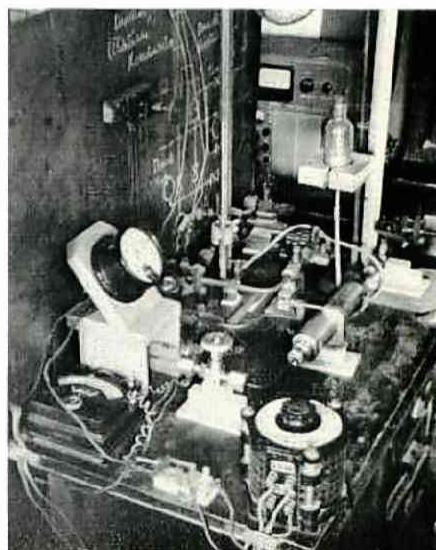
Apparatus for investigation of rate of reaction,
gas and liquid at high pressure—
Laboratory of Physical Chemistry



Apparatus for investigation of
ultra high pressure—
Laboratory of Physical Chemistry



Apparatus for investigation of solubility,
gas and liquid at high pressure—
Laboratory of Physical Chemistry



Apparatus for high pressure explosion,
being manipulated at the right side of
the steel wall protection—
Laboratory of Physical Chemistry

High Pressure Equipments in Abu-yama Seismological Observatory of Kyoto University 25

- Ultra pressure, V The relation between the scale in the Bourdon type pressure gauge and the position of the piston of the intensifier 19, 26 (1945)
- Ultra pressure, VI The measurement of 5,000kg/cm² gas pressure 19, 33 (1945)
- On a membrane pressure gauge 21, 99 (1951)
- On a simplified membrane pressure gauge 24, 81 (1954)

Materials

- The bursting of glass tubes by inner hydrostatic pressure 21, 73 (1951)
- The strength of single crystals of inorganic salts 21, 78 (1951)
- Ultra pressure, VIII Material flow of attachments of high pressure apparatus 20, 73 (1946)

P-V-T Relations

- Ultra pressure, VII The compressibility of the air under ultra pressure 19, 38 (1945)
- The state diagram of 1-butene 19, 43 (1945)
- The state diagram and the critical constants of amylene 21, 50 (1951)
- The state diagram of acetylene 21, 58 (1951)
- The state diagrams of formaldehyde and formaldehyde-acetylene mixtures 22, 13 (1952)
- The state diagrams of benzene-methanol mixtures 23, 35 (1953)
- State diagram of steam 25, 21 (1955)
- On the thermodynamic properties of acetylene under high pressures 25, 25 (1955)
- The compressibility measurements on liquids 23, 20 (1953)

Solubility

- The solubilities of compressed acetylene gas in liquids, I
- The solubility of compressed acetylene gas in water 24, 13 (1954)
- The solubilities of compressed acetylene gas in liquids, II
- The solubility of compressed acetylene gas in methanol 25, 16 (1955)
- The solubilities of compressed acetylene gas in liquids, III
- The solubility of compressed acetylene gas in benzene 25, 52 (1955)
- The solubilities of compressed acetylene gas in liquids, IV
- The solubility of compressed acetylene gas in tetrahydrofuran 26, 1 (1956)

Viscosity

- A new simple viscometer for compressed gases and viscosity of carbon dioxide 21, 63 (1951)
- The viscosity of carbon dioxide, ammonia, acetylene, argon, and oxygen under high pressures 22, 49 (1952)

The viscosity of freons under pressure	24, 74 (1954)
Crystal and Color Center	
The production of single crystals of lithium fluoride	21, 69 (1951)
The production research of single crystals of lithium fluoride	23, 10 (1953)
Electric conductivity of powdered ferroelectric substances under pressures	24, 9 (1954)
The after-effect of hydrostatic pressure on the F-bands in alkali halides	24, 28 (1954)
The after-effect of hydrostatic pressure on the color centers in NaCl	24, 61 (1954)
Effect of plastic deformation upon F-centers in alkali halides	25, 1 (1955)
Effect of plastic deformation upon colloidal centers in NaCl crystal	25, 6 (1955)
The after-effect of hydrostatic pressure on the color centers in alkali halides	25, 10 (1955)
The after-effect of hydrostatic pressure on the silver colloid in silver chloride	25, 41 (1955)
Effect of plastic deformation on color center formation and bleaching in sodium chloride crystal	25, 49 (1955)
Infrared Absorption	
Induced infrared absorption in gaseous acetylene at pressure	24, 49 (1954)
Infrared absorption in gaseous ammonia at pressure	24, 56 (1954)
Measurement of infrared absorption intensity for stretching vibration of carbon disulfide molecule	25, 38 (1955)
Measurement of infrared intensities in tetrafluoroethylene	25, 64 (1955)
Induced infrared absorption in gaseous acetylene at pressure, II	26, 9 (1956)
Colloid	
Distribution of the particles in emulsion prepared by high pressure	21, 82 (1951)
Degradation of polyethylene molecule by high pressure jet	22, 1 (1952)
Degradation of starch by high pressure jet	22, 18 (1952)
Discussion of the distribution of the particles in emulsion prepared by high pressure	22, 46 (1952)
Studies on the intravenous administration of fat emulsion prepared by high pressure jet	22, 83 (1952)
Chemical Reaction	
Reaction between ammonia and carbon dioxide under high pressure	21, 1 (1951)
Equilibrium of urea-water system, I	
The relation between equilibrium pressure and temperature	21, 9 (1951)

High Pressure Equipments in Abu-yama Seismological Observatory of Kyoto University 27

Equilibrium of urea-water system, II

- The relation between equilibrium pressure and packing ratio,
analysis of gas phase, and corrosion of nickel-chrome steel 21, 16 (1951)

Chemical reactions under ultra high pressure,

- Urea synthesis from solid ammonium carbonate 21, 32 (1951)

- Ultra high pressure effect of egg albumin 21, 41 (1951)

- On the air-oxidation of ammonium sulphite crystals under ultra
high pressure 21, 44 (1951)

- Cis-trans isomerization of maleic acid to fumaric acid under pressure 22, 4 (1952)

- The intramolecular rearrangement of β -phenylhydroxylamine to
p-aminophenol under pressure 22, 9 (1952)

Chemical reactions under ultra high pressure,

- Dehydration of salt hydrates 22, 34 (1952)

Chemical reactions under ultra high pressure,

- Reaction between urea and gypsum 22, 39 (1952)

- A note on the stability of ammonium bicarbonate tablets 22, 43 (1952)

- The electrical conductivity of potassium ferrocyanide under pressure 23, 30 (1953)

- Dehydration of pinacol under pressure 23, 38 (1953)

- Polymerization of lower polyoxymethylene glycols under pressure 23, 49 (1953)

- Electrolysis of solid potassium ferrocyanide under pressure 23, 54 (1953)

- The transformation of ammonium thiocyanate into thiourea under
high pressures 24, 1 (1954)

- The reaction between urea and phthalic anhydride under pressure 25, 71 (1955)

Reaction Rate

- Chemical kinetics in the reaction between NH_3 and CO_2 under
pressure 21, 23 (1951)

- Studies on the kinetics of the reaction of acetylene with aqueous
formaldehyde solution, I 22, 22 (1952)

- Studies on the kinetics of the reaction of acetylene with aqueous
formaldehyde solution, II 22, 59 (1952)

- Studies on the kinetics of the reaction of propargyl alcohol with
aqueous formaldehyde solution 23, 73 (1953)

Studies on ethinylation reactions, I

- Synthesis of butynediol in a continuous process 23, 57 (1953)

Studies on ethinylation reactions, II

- Synthesis of propargyl alcohol 23, 66 (1953)

- Synthesis of melamine from urea, I 23, 1 (1953)

- Synthesis of melamine from urea, II 24, 19 (1954)

- Synthesis of melamine from urea, III 24, 67 (1954)

Synthesis of melamine from urea, IV	25, 34 (1955)
Behaviors of acetylene under high pressures in presence of copper or copper alloys	26, 18 (1956)

Explosion

Studies on the explosions under high pressures, I	
The preliminary experiments on the compressions of acetylene and its mixtures with other gases	23, 43 (1953)
Studies on the explosions under high pressures, II	
The explosions of acetylene mixed with oxygen or air and the effects of added substances	24, 41 (1954)
Studies on the explosions under high pressures, III	
The explosions of acetylene mixed with oxygen or air and the effects of pressure and of added substances	25, 58 (1955)

The Review has reported mainly the works of physical chemistry under high pressure. Five years have passed from the alteration of the subject concerning.

The examination of high pressure techniques must be performed. It is sure that the pressure range used exceeds that in literature. On the basis of the accumulated experiences, the new equipments have been constructed with all of the accessories and materials made in Japan. The equipments consist of the groups of the accessories which are easily separable and freely reconstructed (Fig. 1).

Preliminary compressors

The new equipments contain two preliminary compressors for air and oil, the maximum pressures of which are both $1,000 \text{ kg/cm}^2$. The air compressor being order made, consists of four stages, and the oil compressor, having a capacity control device of changing dead space, is made by the laboratory design.

Pipes

The pipes which connect each equipment are examined by bursting pressure tests and their stress-strain relations are measured, considering that almost all of the equipments and pipes, differing in size, are formed cylindrically. The pipes of $1,000 \text{ kg/cm}^2$ working pressure, are 6 mm in inner and 13 mm in outer diameter, and these pipes in the first place are tested by bursting pressure of $1,500 \sim 2,000 \text{ kg/cm}^2$ oil pressure.

Then the pipe chosen freely from the pipes which are passed above tests, is bent to the maximum curvature in use ($r=75 \text{ mm}$), and the strain of the outer diameter due to internal pressure is measured. In measuring the strain, the elements of the strain gauge are pasted on two bends of the pipe, and the changes of the outer diameter of the pipe bent are measured by the changes of the electric

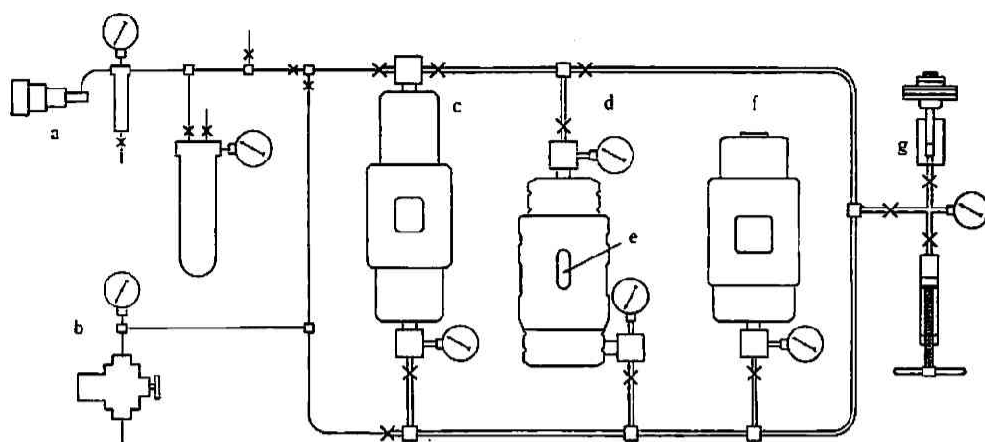


Fig. 1 Installation of the equipments

- a: air compressor
 b: oil compressor
 c: 1st intensifier
 d: 2nd intensifier
 e: high pressure chamber, inner diameter 10~30 mm
 f: high pressure chamber, inner diameter 45 mm
 g: dead weight pressure gauge

resistance of the elements. In the first experiment, the maximum test pressure applied to the pipe is $2,000 \text{ kg/cm}^2$, and maintained for 1 hour, and in the second, up to $2,500 \text{ kg/cm}^2$ and 1 hour as above. Then, in the third experiment, the pipe is ruptured at $2,850 \text{ kg/cm}^2$ to the longitudinal direction at the threaded part for connection, and this ruptured form is the same as observed in the case of the previous bursting tests. The enlargement of the outer diameter of the bend is about 0.01 mm at $2,800 \text{ kg/cm}^2$, and the linear stress-strain relation holds and is reproducible up to the bursting pressure observed. After the bursting test, thin fragments are found which are certainly stripped from the inner wall of the bending parts of the pipe.

The tests of the pipes using over $1,000 \text{ kg/cm}^2$ and of the cylindrical equipments are performed as follows.

The following three samples are examined where A is carbon steel, B nickel-chrome steel and C carbon-vanadium steel. The compositions of the steels are shown in the table.

	C	Si	Mn	P	S	Ni	Cr	Mo	V
A	0.75	0.22	0.32	0.014	0.013	0.08	0.08	0.02	—
B	0.32	0.26	0.57	0.009	0.010	3.00	0.35	0.25	—
C	0.82	0.13	0.16	0.005	0.007	—	—	—	0.16

These pipes are of 19 mm outer diameter and of hexagonal form where the distance between the opposite planes is 22 mm, when originally formed as pipes. The original pipes and those finished in 13 and 16 mm outer diameter are used as

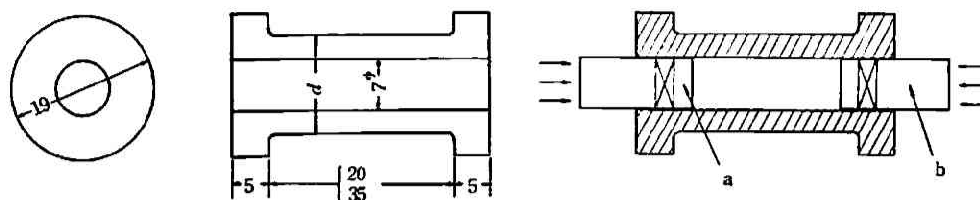


Fig. 2 Pipe and arrangement on testing
a: Bridgman's plug b: piston

the samples for pressure test (Fig. 2). In either case, the inner wall is finished in 7 mm diameter by reamer within 2/100~3/100 mm unevenness.

In the procedure of testing, the pressure is increased at constant rate and the extension of inner wall is measured after releasing of pressure.

In the cases of higher pressure, the pressure proof cannot be attained by using the sealing of Bridgman type owing to the extension of inner wall, and the pipes of the sample are often ruptured axially. The extension of inner wall when pressure proof breaks is not always constant but has relations to the pressure. The lengths of the pipes used are 45 and 35 mm, and the difference due to the length is not observed in the present testing. The reason may be understood from the following facts. In the rupture of pipes or the bursting of Bridgman type sealing, the maximum extension of inner wall is found at the middle part of the pipes and the extension

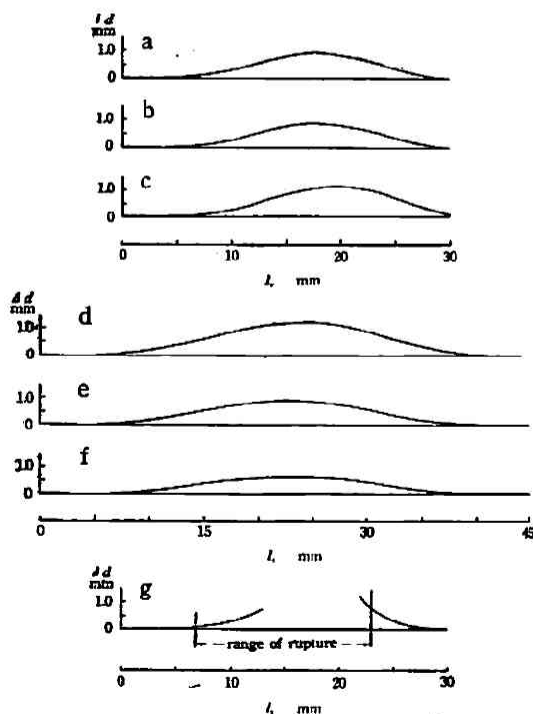


Fig. 3 Permanent deformation in inner diameter

	material	outer diameter mm	pressure at which sealing breaks kg/cm ²	
a:	A	13	6500	} pipe length 30 mm
b:	A	16	8600	
c:	A	19	14600	
d:	A	13	6500	} pipe length 45 mm
e:	A	16	7900	
f:	A	19	9200	
g:	B	13	8300	bursting example

Δd : deformed amount in inner diameter

l : distance from one end of pipe for testing

at the end is converging to zero in either case. The extension is symmetrical with a center at the maximum extension as shown in Fig. 3.

The permanent strain and the rupture due to pressure are examined as mentioned above. The range of permanent strain due to internal pressure is determined from

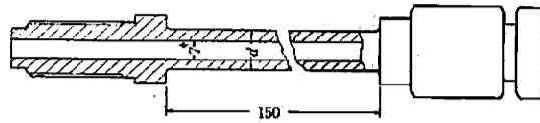


Fig. 4 Pipe for testing by strain meter

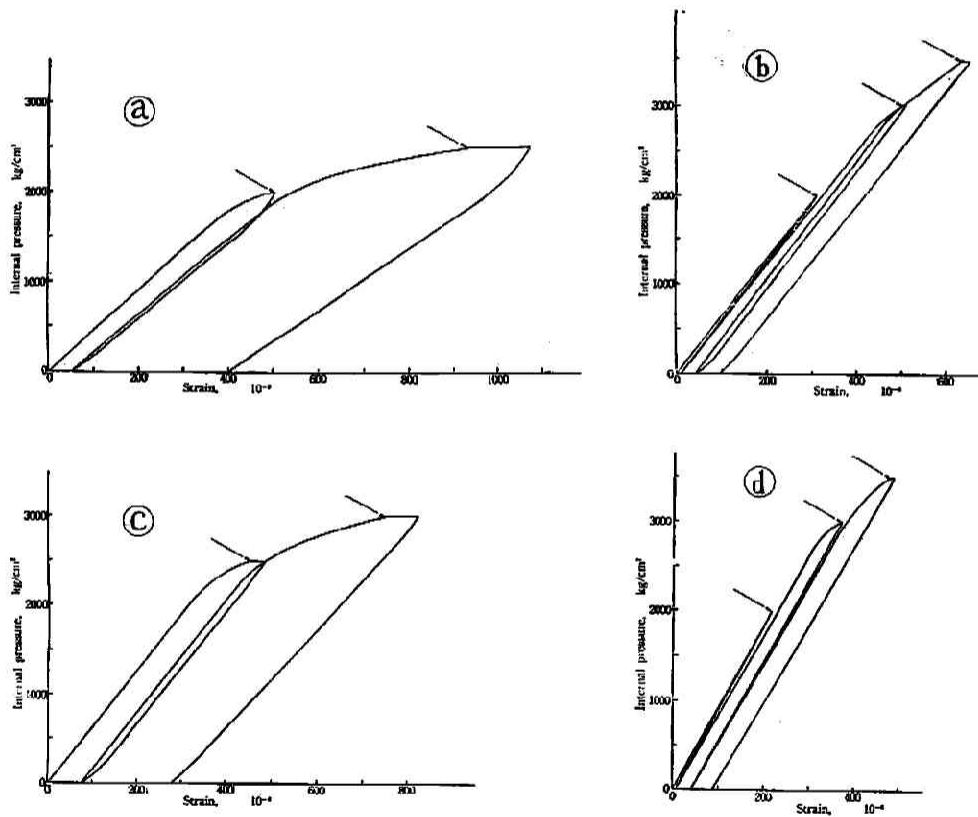


Fig. 5 Stress-strain relations showing linearity and flow

	material	outer diameter mm
a	C	13
b	A	13
c	C	16
d	A	16

The starting points of flow by keeping for 1 hour at the pressure are shown by arrows.

the limit of linearity in stress-strain relations (the reproducible limit). The pipes for testing are similar to those shown in Fig. 4, but the length is much longer and the inner diameter is 6 mm. The pipe has a connection to high pressure apparatus at one end and is closed at the other.

The extension of the outer diameter of pipes (6 mm in inner diameter, 13 and 16 mm in outer diameter, d) is plotted against pressure from the measurements by means of strain gauge of which element is pasted at the middle part of pipes. In the first stage, the stress-strain relations are linear, and over a certain pressure the strain becomes much higher to slight pressure change, and then the pipe is ruptured finally.

The range of linearity becomes longer for the pipes of greater strength and larger thickness (Fig. 5). The pressure yielding a finite strain is the measure of the strength of materials. The strength of pipes can be examined by the amount in outer diameter deformed by the maximum pressure in the linearity range, from which the amount deformed in inner diameter can be calculated.

The pressure is released at the pressure slightly over the maximum pressure in the linearity range. (The permanent strain is found by keeping for a certain time at the pressure.) And further pressurizing, the range of the linearity is extended, that is the effect of stretching. The pipes which have 13 and 16 mm outer diameter and are made with the materials A and C are examined by pressurizing and releasing stepwise up to 1000, 2000, 3000, 3500 and 4000 kg/cm² respectively. The stress-strain relations are shown in the figure from which the effect of stretching may be understood (Fig. 6).

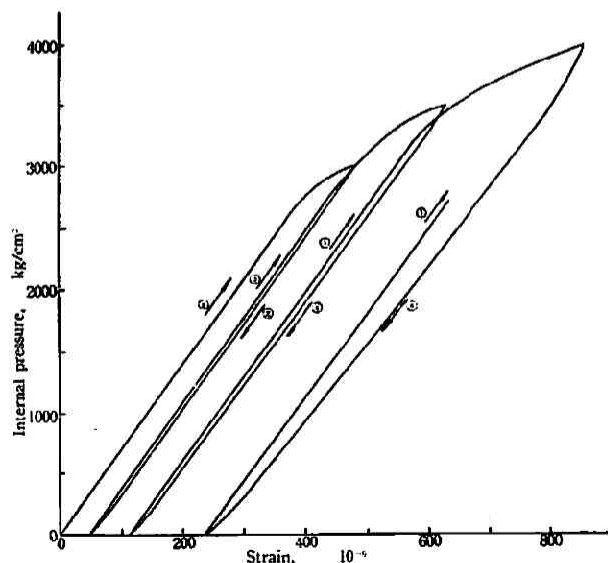


Fig. 6 Stress-strain relation
showing stretching effect

material A
outer diameter 16 mm

The pressure durability of the pipes is determined by the length and slope of the linear range in either case.

The maximum stress in inner wall corresponding to the maximum internal pressure can be obtained from these relations. Considering that the stress yields flow without its dependence on thickness when it reaches a definite limit, the maximum stresses of A, B and C may be obtained. In either case, these values of the maximum pressure corresponding to maximum stress measured agree with those calculated from the maximum stress given to the materials.

The values of the maximum pressure (kg/cm^2), neglecting the effect of stretching, are shown in the table.

	13 ϕ	16 ϕ	19 ϕ	hexagonal*
A	2200	2550	2780	2970
B	4220	4890	5330	5700
C	1750	2070	2210	2370

* The distance between the opposite planes is 22 mm.

From the facts mentioned above, the working pressure can be determined.

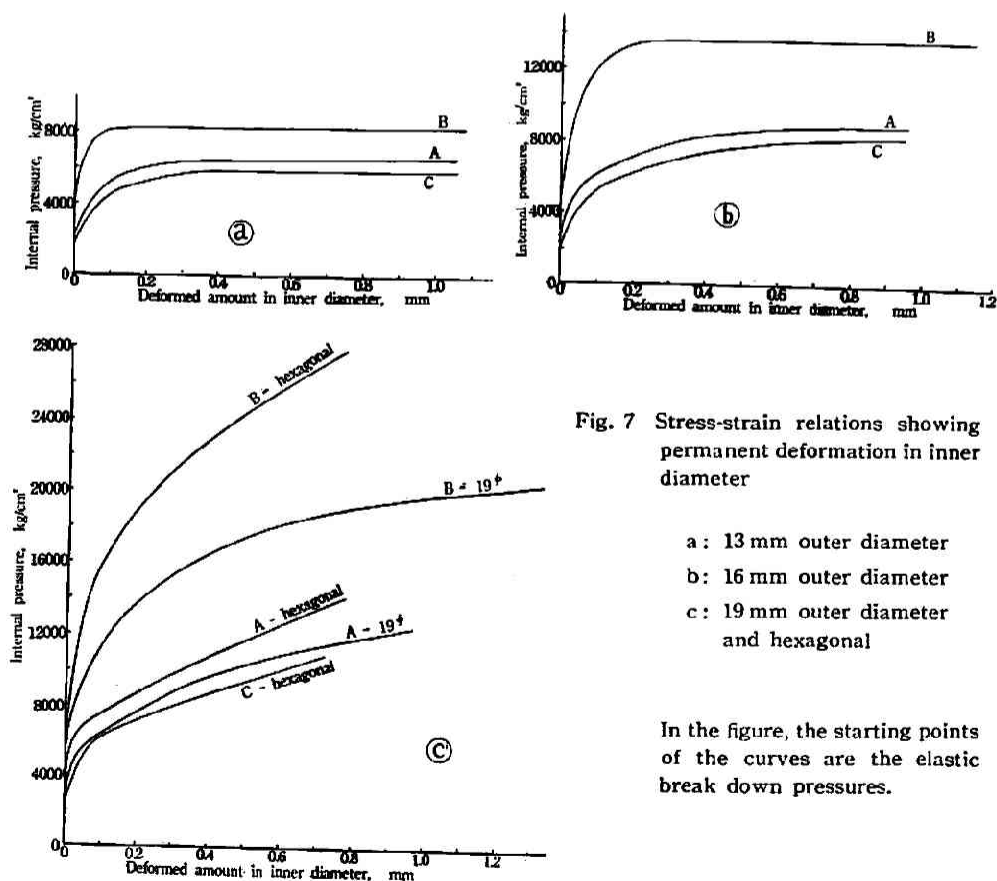


Fig. 7 Stress-strain relations showing permanent deformation in inner diameter

- a : 13 mm outer diameter
- b : 16 mm outer diameter
- c : 19 mm outer diameter and hexagonal

In the figure, the starting points of the curves are the elastic break down pressures.

The relation between internal pressure and strain (permanent and causing to rupture) is shown in the above figures for the pipes, hexagonal and cylindrical of 13, 16 and 19 mm in diameter, and of the materials A, B and C. These figures are plotted from the experimental values and from those estimated (Fig. 7).

Intensifiers

The intensifier consists of two stages as shown in Fig. 1, each having the same construction and being composed of three pieces, that is, an upper chamber to which the pressure of $1,000 \text{ kg/cm}^2$ is transmitted from the preliminary air compressor, a lower chamber to which the hydrostatic pressure of $1,000 \text{ kg/cm}^2$ is transmitted from the oil compressor, and a composed piston which is mounted between the upper and lower chambers, whose part of the smaller diameter is in contact with air and the other part of the larger diameter with oil. The pressure of the air is intensified by the operation of the composed piston which is moved by compressing the oil into the intensifier with the oil compressor and then the compressed air is introduced into the upper chamber of the intensifier in the second stage, where the air is compressed to still higher pressures. The intensifiers are made of nickel-chrome steel with heat treatment, each weight being 800 kg. The chamber *e* in Fig. 1 consisting of a cylinder-piston system in which the maximum pressure is obtained, is mounted between the two composed pistons of the intensifier in the second stage and is doubled, its outer part being made of nickel-chrome steel with heat treatment and its inner piston cylinder made of high speed cutting metal or cobalt cemented tungsten carbide. A pressure of $40,000 \text{ kg/cm}^2$ may be reached with the intensifier thus designed even with the above mentioned hard metals of 3 cm in inner diameter. Each kind of hard metals of 1~3 cm in diameter is provided. The high pressure

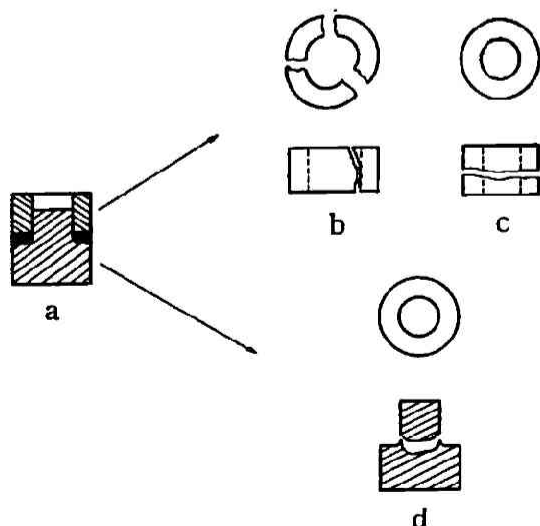


Fig. 8 Rupture of Bridgman's plug

- a: plug construction
- b: ring broken radially
- c: ring broken annularly
- d: mushroom broken at neck

cylinder of high speed cutting metal exposed to the pressure of 20,000~30,000 kg/cm² shows considerable permanent deformation, though the cylinder is tightened mechanically with the outer cylinder, whereas the cylinder and piston of tungsten carbide do not deform in this range of pressure but sometimes the Bridgman's plug suffers deformation. The boss of the plug in mushroom shape is sometimes parted as shown in the above Fig. 8. This sort of damage is also often found at the cylinder of high speed cutting metal with heat treatment exposed to the pressure of 10,000~30,000 kg/cm² and at this test the ring fitted in the cylinder is sometimes ruptured radially and sometimes torn into two.

The upper chamber of *f* in Fig. 1 which is packed with pressure transmitting oil and may be used as an intensifier, is adapted to various kinds of experiments at the pressures of several thousands kilograms per square centimeter by the change of the attachment to the upper double cylinder, its inner diameter being 45 mm.

The measurements of pressures

A dead weight pressure gauge is used for the measurement of pressures, its maximum pressure being 3,000 kg/cm² and its sensibility 1/10 kg/cm². The pressure of the high pressure side is calculated from that of the low pressure side, that is the oil side, measured with the dead weight pressure gauge and a Bourdon type pressure gauge.

The experiments on the demonstration by means of the new equipments will be mentioned.

Effect of plastic deformation upon colloidal centers in sodium chloride crystal

In the previous paper¹⁾ it has been shown that NaCl crystals containing colloidal centers became dichroic when the crystal was deformed plastically at a pressure of 5,000 kg/cm² and the dichroism disappeared when the deformed crystal was annealed at 200°C. The present investigation is undertaken to study the dichroism which the die-casting with higher pressures such as 20,000 and 30,000 kg/cm² causes in NaCl crystals containing colloidal centers and at the same time to test newly constructed high pressure equipments, especially high pressure vessels.

Colloidal centers are produced in NaCl crystal by annealing crystals containing F-centers at 400°C for about 20 minutes and rapid quenching. However a simple bell-shaped colloidal band is not formed in the crystals and moreover the colloidal bands of two crystals have the band peaks at the different wavelength such as 578 and 555 mμ depending on the crystal sizes because of the difficulty of sufficiently rapid quenching for large crystals used in this experiment. The former

1) R. Kiyama and F. Okamoto, *This Journal*, 25, 6 (1955)

is used in the experiment of $20,000 \text{ kg/cm}^2$ and the latter in the experiment of $30,000 \text{ kg/cm}^2$. The samples suitable for experiments are cleaved from the inner region of the colored crystals. The same procedure and technique as in the previous experiment¹⁾ are used for the absorption measurements.

Exp. 1 The plastic deformation is carried out by die-casting at room temperature as follows. The colored crystal cleaved to a cubic form of $12.5 \times 14.0 \times 14.5 \text{ mm}$ is placed in the cylindrical pressure vessel made of cobalt cemented tungsten carbide and is deformed to a cylindrical form of 20 mm in diameter and 8.0 mm in thickness by the stepwise compression of $8,000 \text{ kg/cm}^2$ for 5 minutes, $16,000 \text{ kg/cm}^2$ for 5 minutes and finally $20,000 \text{ kg/cm}^2$ for a few seconds. For the purpose of the measurement of the absorption spectra, two plates with a thickness of 4.0 mm are cut from the deformed crystal along the plane normal or parallel to the direction of compression respectively, and are used to determine the absorption spectra. The first measurement of the absorption spectrum is carried out after 1 day storage in the dark instead of the measurement immediately after releasing pressure. The plastic deformation shifts the colloidal band to longer wavelength side (from 578 to $612 \text{ m}\mu$) when measured parallel to the direction of compression. On the other hand the band peak measured

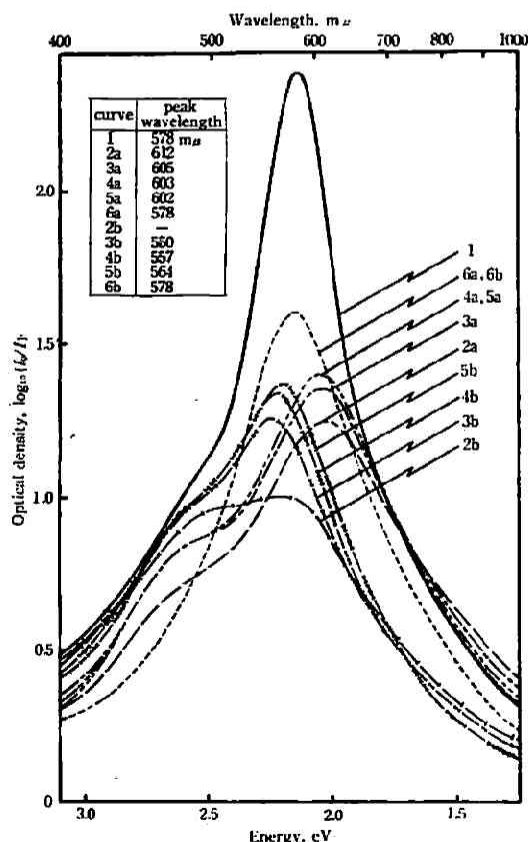


Fig. 9 Changes of the absorption spectrum of colloidal centers in NaCl crystal after plastic deformation. Measurements in the respective directions parallel and normal to the compression. pressure = $20,000 \text{ kg/cm}^2$, crystal thickness = 4.0 mm

1: absorption spectrum of the crystal measured previous to plastic deformation

2a and 2b: after 1 day storage in the dark

3a and 3b: after 5 days storage

4a and 4b: after 14 days storage

5a and 5b: after 29 days storage

6a and 6b: after 30 minutes annealing at 200°C

a and b indicate the measurements in the directions parallel and normal to the compression respectively.

normal to the direction of compression locates at shorter wavelength side than the initial location, but the peak wavelength is hardly determined because of its broad band peak. Storage in the dark shifts each band back towards $578\text{ m}\mu$. Annealing at 200°C for 30 minutes makes the parallel and normal spectra identical, and both band peaks return to $578\text{ m}\mu$ of the initial location. These changes of absorption spectra are shown in Fig. 9.

Exp. 2 The colored crystal cleaved to a cubic form of $13.8\times13.8\times5.0\text{ mm}$ is placed in the cylindrical pressure vessel made of high speed cutting metal and is deformed to a cylindrical form of 20 mm in diameter and 3.0 mm in thickness at a pressure of $30,000\text{ kg/cm}^2$ for 5 minutes and then the deformed crystal is kept in the pressure vessel for 14 days. For the purpose of the measurement of the absorption spectra, a plate with a thickness of 2.3 mm is cut from the deformed crystal along the plane normal to the direction of compression and is used to determine the absorption spectra parallel to the direction of compression. In this case the absorption spectrum normal to the direction of compression is not determined because the deformed crystal is too thin to be cut as the absorption specimen. The plastic deformation shifts the colloidal band from $555\text{ m}\mu$ to $614\text{ m}\mu$. Storage in the dark shifts the band back towards $555\text{ m}\mu$. When the deformed crystal is annealed at 200°C for 30 minutes the peak wavelength returns to $555\text{ m}\mu$ of initial location. These changes of absorption spectra are shown in Fig. 10.

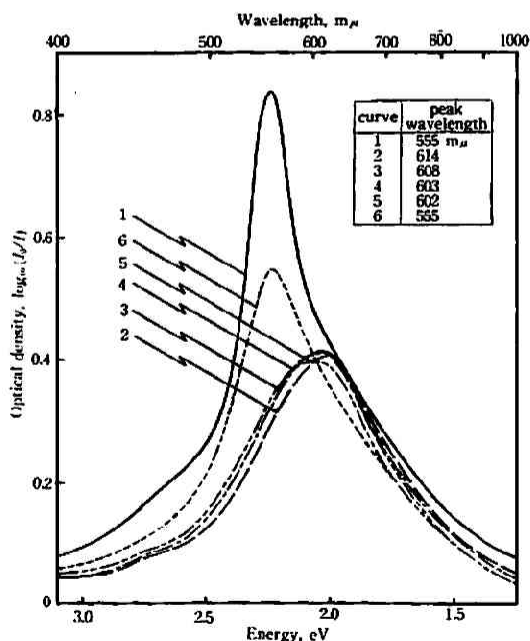


Fig. 10 Changes of the absorption spectrum of colloidal centers in NaCl crystal after plastic deformation. Measurements in the direction parallel to the compression.

pressure = $30,000\text{ kg/cm}^2$,
crystal thickness = 2.3 mm

- 1: absorption spectrum of the crystal measured previous to plastic deformation
- 2: after 1 day storage in the dark
- 3: after 5 days storage
- 4: after 14 days storage
- 5: after 29 days storage
- 6: after 30 minutes annealing at 200°C

These experimental results are summarized as follows. (1) The plastic deformation at a pressure of 20,000 or $30,000\text{ kg/cm}^2$ makes the crystal containing colloidal

centers dichroic in the same manner as the result of the previous experiment at a pressure of $5,000 \text{ kg/cm}^2$. (2) The amount of the peak shift of colloidal band in the present experiments can not be compared strictly with the previous experimental results because of the differences in the initial peak wavelength of the colloidal band, pressing procedure, pressing time and time interval of absorption measurements taken after deformation, whereas the ratio of the crystal thickness after deformation to that before is in the range of $0.55 \sim 0.60$ as in the previous experiment. On the whole it may be considered that the amount of peak shift is greater in the crystal deformed with higher pressure. (3) When the crystal containing colloidal centers is deformed, the crystal becomes dichroic and when the deformed crystal is annealed, the dichroism disappears. The results indicate that all the spherical colloidal particles are deformed essentially to the same ellipsoidal shape by uniaxial compression and the deformed colloidal particles recover during storage and annealing as illustrated in the previous paper. Moreover on the basis of the experimental results, it may be considered that the higher pressure causes a greater deformation of colloidal particles and in consequence the greater peak shift.

Studies on compacted powder crystals

In the Laboratory of Physical Chemistry, we have been studying on fabrication of compacted optical crystals of alkali and silver halides. Now the preparation of scintillation crystals has been attempted using high pressure compaction technique, and satisfactorily clear and luminescent phosphors have been obtained for thallium activated alkali iodides. The compacted scintillation crystals are prepared as follows. For example, potassium iodide powders activated by $0.01 \sim 1.00\%$ of thallous iodide are subjected to compaction pressure of $2,000 \sim 10,000 \text{ kg/cm}^2$ in a specially designed pressure vessel from which the air can be withdrawn by a vacuum pump. Pressure is held for $5 \sim 180$ minutes after evacuation for $5 \sim 60$ minutes. Clear and luminescent cylindrical disks are obtained in some instances with diameter of 10 mm and thickness of $2 \sim 8 \text{ mm}$. Longer pressing times, higher pressures and higher evacuations make the compacted crystals more transparent and the crystals remain transparent for longer periods of time. Further work is undertaken to investigate the effect of pressure on the quality of compacted optical crystals and compacted scintillation crystals.

Polymorphic transition of thallous iodide under pressure

It is known that TII has a transition from low temperature form (yellow) to high temperature form (red) at atmospheric pressure at about 170°C . We have observed that TII undergoes a transition from yellow to red at about $5,000 \text{ kg/cm}^2$ at room temperature. This transition under pressure is investigated by measuring the absorption spectra of the disks made by the high pressure compaction technique used

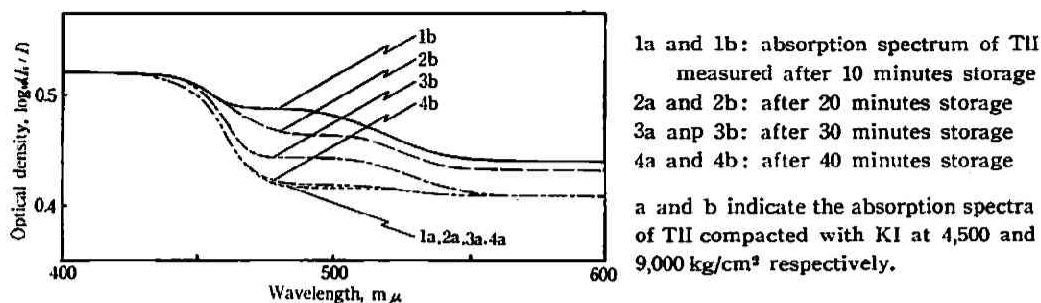


Fig. 11 Changes of the absorption spectrum of TII compacted with KI at 4,500 and 9,000 kg/cm². TII content in KI=1.0%, thickness=0.4 mm

in the preceding experiment. Potassium iodide containing 1.0% of TII is ground to 200 mesh or better, and 100 milligrams of the mixture are placed in the cylindrical pressure vessel and pressed to a definite pressure after evacuation. The resulting disks of 20 mm in diameter and about 0.4 mm in thickness are fairly clear masses colored in yellow or red depending on the applied pressure. The transition from yellow to red is observed at about 5,000 kg/cm². The red form obtained at high pressure gradually discolors to yellow form after releasing pressure but in this case the rate of the discoloration is slower than that in the case of pure TII. The slow discoloration makes it possible to measure the absorption spectra of high pressure form after releasing pressure. Generally the disks compacted at higher pressure show slower discoloration. Changes of the absorption spectra of the TII compacted with KI at 4,500 and 9,000 kg/cm² are shown in Fig. 11. The results reveal that the red form obtained at 9,000 kg/cm² has an increased absorption in the range of 460~520 mμ and the increased absorption almost disappears within about 40 minutes after releasing pressure. The slow discoloration of high pressure form of TII compacted with KI may be ascribed to the reason that the high pressure form of TII is obstructed to change into a low pressure form by surrounded compacted KI. Further experiments are undertaken to determine the transition pressure of pure TII and to investigate the effect of KI on the transition pressure of TII.

*The Laboratory of Physical Chemistry,
 Kyoto University*